

1 S-matrix and amplitude \mathcal{M}

Statement: Given a theory (e.g. defined by Lagrangian), S-matrix is a matrix which contains information about all processes that can proceed in that theory, such as $2 \rightarrow 2$, $2 \rightarrow 3$, $2 \rightarrow 4$ etc. plus the time-reversed processes. When dealing with unitarity limits, we usually limit our attention to $2 \rightarrow 2$ processes and out of these only to the most 'prominent' ones. As an example I show the 'prominent' part of the S-matrix for our ρ resonance model:

$$S = \begin{matrix} & \pi^+\pi^- & tt(++) & tt(--) & tt(+-) & tt(-+) \\ \pi^+\pi^- & \left(\begin{matrix} S^{00} & S^{++} & S^{--} & S^{+-} & S^{-+} \\ S^{++} & S^{++++} & S^{+---} & S^{+--+} & S^{+--+} \\ S^{--} & S^{--++} & S^{----} & S^{--+-} & S^{----} \\ S^{+-} & S^{+---} & S^{+---} & S^{+--+} & S^{+--+} \\ S^{-+} & S^{-+++} & S^{-+++} & S^{-+++} & S^{-+++} \end{matrix} \right) \end{matrix} \quad (1)$$

Here, e.g., S^{++++} contains information about process $t\bar{t} \rightarrow t\bar{t}$ in which initial helicities for the top-antitop quark pair are $(++)$ respectively and final helicities are $(+-)$.

S-matrix is unitary (the usual argument is that this follows from probability conservation):

$$SS^\dagger = 1 \quad (2)$$

We must remember though that the unitarity condition holds for the complete S-matrix, not just the 'prominent' part shown in Eq. 1.

In calculations, we usually do not deal with the S-matrix itself but rather with amplitude \mathcal{M} . The relation between \mathcal{M} and S depends on the particular representation we choose for the S-matrix elements. The usual choice is 'momentum representation'. I suppose this means that initial and final states are described by eigenfunctions of 4-momentum. Here the relation between S and \mathcal{M} is given by (S^{ij} is one of S-matrix elements - for example, for Eq. 1 we have $S^{22} = S^{++++}$)

$$S^{ij} = 1 - (2\pi)^4 \delta^{(4)}(P_f - P_i) \mathcal{M}^{ij} \quad (3)$$

with P_f, P_i total final and initial 4-momenta.

Another choice is 'angular momentum representation' with initial and final states described by eigenfunctions of angular momentum. Here the relation between S and \mathcal{M} is given by (for this and many of the points made in this section see [1])

$$S_J^{ij} = 1 + 2i\mathcal{M}_J^{ij} \quad (4)$$

The subscript J indicates angular momentum representation. In this representation we call the amplitude 'partial wave' amplitude. I believe the S-matrix is

now of the form

$$S = \begin{pmatrix} S_0 & 0 & 0 & 0 & \dots \\ 0 & S_1 & 0 & 0 & \dots \\ 0 & 0 & S_2 & 0 & \dots \\ \dots & & & & \dots \end{pmatrix} \quad (5)$$

with S_J denoting S-matrix for the J th partial wave. The advantage (!) of this representation is that each S_J is itself unitary:

$$S_J S_J^\dagger = 1 \quad (6)$$

and we can have unitarity constraints for each partial wave amplitude.

The relation between amplitude \mathcal{M} and \mathcal{M}_J is given by the expansion of \mathcal{M} into partial waves as follows (I use here partial waves a_J as intermediate step since a_J are often used in literature)

$$\mathcal{M} = 16\pi \sum_J (2J+1) d_{\lambda\mu}^J a_J \quad (7)$$

where

$$a_J = \frac{1}{2} \sqrt{\frac{s}{p_f p_i}} \mathcal{M}_J, \quad (8)$$

$d_{\lambda\mu}^J$ are Wigner's functions, $\lambda = \lambda_1 - \lambda_2, \mu = \lambda_3 - \lambda_4$ with λ_i helicities of the $1+2 \rightarrow 3+4$ process. For high energies the initial p_i and final p_f momenta behave as $p_i, p_f \rightarrow \frac{1}{2}\sqrt{s}$ and

$$a_J \rightarrow \mathcal{M}_J \quad (9)$$

To obtain partial waves \mathcal{M}_J from the amplitude \mathcal{M} we use

$$\mathcal{M}_J = \frac{1}{32\pi} \sqrt{\frac{4p_f p_i}{s}} \int_0^\pi d_{\lambda\mu}^J \mathcal{M} \sin \theta d\theta \quad (10)$$

In the case of identical particles in initial and/or final state the above relation picks up an additional factor of $\frac{1}{\sqrt{2}}$ for each pair of identical particles [1].

To conclude this section we write down the differential cross section for the amplitude \mathcal{M} :

$$\frac{d\sigma}{d\Omega} = \frac{1}{64\pi^2 s} \frac{p_f}{p_i} |\mathcal{M}|^2 \quad (11)$$

Another convenient choice for the amplitude (see [1, 2]) is one in which the differential cross section is given by

$$\frac{d\sigma}{d\Omega} = |f|^2 \quad (12)$$

where

$$f = \frac{1}{8\pi\sqrt{s}} \sqrt{\frac{p_f}{p_i}} \mathcal{M} \quad (13)$$

and

$$f = \frac{1}{p_i} \sum_J (2J+1) d_{\lambda\mu}^J \mathcal{M}_J \quad (14)$$

2 Unitarity limits on partial waves \mathcal{M}_J

To derive unitarity limits on partial waves we go back to Eq. 4 and express \mathcal{M}_J^{ij}

$$\mathcal{M}_J^{ij} = \frac{1}{2i}(S_J^{ij} - 1), \quad (15)$$

after squaring we get

$$\begin{aligned} |\mathcal{M}_J^{ij}|^2 &= \frac{1}{2i} \frac{1}{(-2i)} (S_J^{ij} - 1)(S_J^{ij*} - 1) \\ &= \frac{1}{4} (|S_J^{ij}|^2 - 2\text{Re} S_J^{ij} + 1) \end{aligned} \quad (16)$$

Using $S_J S_J^\dagger = 1$ we can write

$$S_J^{ij} S_J^\dagger{}^{jk} = S_J^{ij} S_J^{kj*} = 1 \quad (17)$$

Thus for the i -th diagonal term we have

$$\sum_j S_J^{ij} S_J^{ij*} = |S_J^{i1}|^2 + |S_J^{i2}|^2 + |S_J^{i3}|^2 + \dots = 1 \quad (18)$$

hence for any i, j we have

$$|S_J^{ij}|^2 < 1 \quad (19)$$

Further,

$$\begin{aligned} |S_J^{ij}|^2 &= (\text{Re } S_J^{ij} + i\text{Im } S_J^{ij})(\text{Re } S_J^{ij} - i\text{Im } S_J^{ij}) \\ &= (\text{Re } S_J^{ij})^2 + (\text{Im } S_J^{ij})^2 < 1, \end{aligned} \quad (20)$$

hence

$$|\text{Re } S_J^{ij}| < 1 \quad (21)$$

Going back to Eq. 16, and taking into account Eqs. 19,21, we conclude that ($0 \leq |S_J^{ij}|^2 \leq 1$, $-2 \leq 2\text{Re } S_J^{ij} \leq 2$)

$$0 \leq |\mathcal{M}_J^{ij}|^2 \leq 1 \quad (22)$$

Thus, each partial wave is bounded by

$$|\mathcal{M}_J^{ij}| \leq 1 \quad (23)$$

Often in the literature one finds a little bit different treatment of unitarity limits. Instead of placing a separate limit on each element of the partial wave matrix \mathcal{M}_J as in the equation above, one chooses to diagonalize the partial wave matrix (the 'prominent' part of it, in our case the part corresponding to Eq. 1 via Eq. 4) and demands that the largest eigenvalue be less than one. This

general condition is derived in the Appendix of Ref. [1]. These two different treatments should lead to similar bounds on the coupling constants - if not, we would have a problem. I have not used the latter approach in this work.

If the partial wave violates the limit of Eq. 23 at some energy, the usual conclusion is that the amplitude \mathcal{M} as found from tree-level Feynman diagrams of a renormalizable theory is not complete and we need to include terms beyond the tree level to get the partial wave obeying the unitarity limits. Or, if we do not have a renormalizable theory, we have to include some new physics (new particle) at that energy, which would unitarize the amplitude. This speculation proved to be very fruitful in the history of particle physics, see e.g. Ref. [2].

To conclude this section, I would like to note that Horejsi in Ref. [2] makes distinction between elastic and inelastic unitarity bound. The limit of Eq. 23 is general and thus applies to both cases. However, for inelastic processes I can imagine that Eq. 15 simplifies to

$$\mathcal{M}_J^{ij} = \frac{1}{2i} S_J^{ij}, \quad (24)$$

which means that if we limit ourselves to inelastic processes we in fact discard the part of S-matrix which says that there is nonzero probability that nothing happens ($1+2 \rightarrow 1+2$). This, of course, includes unity matrix of Eq. 15. Now, using Eq. 19 we have for inelastic case

$$|\mathcal{M}_J^{ij}| \leq \frac{1}{2} \quad (25)$$

3 Unitarity limits in ρ -resonance models. TopBESS notation.

The most natural Lagrangian we can write down for interactions of V^0 resonance with scalar pions is

$$\mathcal{L}_{V^0\pi\pi} = +ig_\pi \frac{M_{V^0}}{v} (\pi^- \partial^\mu \pi^+ - \pi^+ \partial^\mu \pi^-) V_\mu^0 \quad (26)$$

where in topBESS

$$g_\pi = \frac{M_{V^0}}{v} \frac{1}{g''} \quad (27)$$

For the charged V^+ resonance we have

$$\mathcal{L}_{V^+\pi\pi} = -ig'_\pi \frac{M_{V^+}}{v} (\partial^\mu \pi^- \pi^0 - \pi^- \partial^\mu \pi^0) V_\mu^+ \quad (28)$$

where in topBESS

$$g'_\pi = \frac{M_{V^+}}{v} \frac{1}{g''} \quad (29)$$

For the Vff -Lagrangian we can write

$$\mathcal{L}(V^0) = g_V^t \bar{t} \gamma^\mu t V_\mu^0 + g_A^t \bar{t} \gamma^\mu \gamma^5 t V_\mu^0 \quad (30)$$

$$g_V^b \bar{b} \gamma^\mu b V_\mu^0 + g_A^b \bar{b} \gamma^\mu \gamma^5 b V_\mu^0 \quad (31)$$

$$\mathcal{L}(V^\pm) = g_V^{tb} \bar{t} \gamma^\mu b V_\mu^\pm + g_A^{tb} \bar{t} \gamma^\mu \gamma^5 b V_\mu^\pm + h.c. \quad (32)$$

where in topBESS (using Eqs. 406, 408 in topBESS notes and neglecting mixing of V with A, Z)

$$g_V^t = -b_R \frac{g''}{8} - b_L \frac{g''}{8}, \quad g_A^t = -b_R \frac{g''}{8} + b_L \frac{g''}{8} \quad (33)$$

$$g_V^b = +p^2 b_R \frac{g''}{8} + b_L \frac{g''}{8}, \quad g_A^b = +p^2 b_R \frac{g''}{8} - b_L \frac{g''}{8} \quad (34)$$

$$g_V^{tb} = -p b_R \frac{g''}{4\sqrt{2}} - b_L \frac{g''}{4\sqrt{2}}, \quad g_A^{tb} = -p b_R \frac{g''}{4\sqrt{2}} + b_L \frac{g''}{4\sqrt{2}} \quad (35)$$

Important partial widths in the limit $m_t, m_b \rightarrow 0$ are given as

$$\Gamma(V^0 \rightarrow tt) = \frac{M_{V^0}}{4\pi} (g_V^t{}^2 + g_A^t{}^2) \quad (36)$$

$$\Gamma(V^0 \rightarrow bb) = \frac{M_{V^0}}{4\pi} (g_V^b{}^2 + g_A^b{}^2) \quad (37)$$

$$\Gamma(V^0 \rightarrow \pi^+ \pi^-) = \frac{4g_\pi^2}{192\pi} \frac{M_{V^0}^3}{v^2} \quad (38)$$

$$\Gamma(V^+ \rightarrow tb) = \frac{M_{V^+}}{4\pi} (g_V^{tb2} + g_A^{tb2}) \quad (39)$$

$$\Gamma(V^+ \rightarrow \pi^+ \pi^0) = \frac{4g_\pi'^2}{192\pi} \frac{M_{V^+}^3}{v^2} \quad (40)$$

I will study unitarity limits in the following scenarios:

Scenario 1) $p = 1, b_L = 0$ limit

It follows that

$$\begin{aligned} g_V^t &= g_A^t = -b_R \frac{g''}{8} \\ g_V^b &= g_A^b = +b_R \frac{g''}{8} \\ g_V^{tb} &= g_A^{tb} = -b_R \frac{g''}{4\sqrt{2}} \end{aligned} \quad (41)$$

Scenario 2) $p = 1, b_L = b_R = b$ limit

It follows that

$$g_A^t = 0, \quad g_V^t = -b \frac{g''}{4}$$

$$\begin{aligned}
g_A^b &= 0, & g_V^b &= +b \frac{g''}{4} \\
g_A^{tb} &= 0, & g_V^{tb} &= -b \frac{g''}{2\sqrt{2}}
\end{aligned} \tag{42}$$

Scenario 3) $p = 0, b_L = 0$ limit

$$\begin{aligned}
g_V^t &= g_A^t = -b_R \frac{g''}{8} \\
g_V^b &= g_A^b = 0 \\
g_V^{tb} &= g_A^{tb} = 0
\end{aligned} \tag{43}$$

3.1 $\pi^+\pi^- \rightarrow \pi^+\pi^-$

The amplitude for $\pi^+\pi^- \rightarrow \pi^+\pi^-$ is the sum of three terms, s-channel V^0 exchange (see my notes 12.2.98), t-channel V^0 exchange (see my notes 3.2.04) and 4-point vertex (see, e.g., D. Dominici, hep-ph/9711385, Eqs. 6,7 - $\mathcal{M}_{4\text{-vertex}} = \frac{s+t}{v^2} = \frac{s}{2v^2}(1 + \cos\theta)$):

$$\begin{aligned}
\mathcal{M} &= g_\pi^2 \frac{M_{V^0}^2}{v^2} \frac{s \cos\theta}{s - M_{V^0}^2 + iM_{V^0}\Gamma_{V^0}} \\
&+ g_\pi^2 \frac{M_{V^0}^2}{v^2} \frac{s + s/2(1 + \cos\theta)}{-s/2(1 - \cos\theta) - M_{V^0}^2} \\
&+ \frac{s}{2v^2}(1 + \cos\theta)
\end{aligned} \tag{44}$$

Partial waves and unitarity limits can be found in melo/SERVER/FYZIKA/MATHEMATICA/PARTIALWAVE/2010/pipi-pipi-gama1-2010-*.nb where * stands for a,a1,a2,a3 (scenario 1),b,b1,b2,b3 (scenario 2),c,c1,c2,c3 (scenario 3).

Scenario 1 ($M_{V^0} = 1$ TeV). For $g_V^t = g_A^t = 0.2, g_V^b = g_A^b = -0.2$ we get a contour plot of a_0 partial wave in Fig.1a and a contour plot of a_1 partial wave in Fig.1b. If we demand that the amplitude be unitary up to $\sqrt{s} = 3$ TeV, we get from Fig.1a

$$0.6 \leq g_\pi \leq 1.4, \tag{45}$$

or if we demand that the amplitude be unitary up to $\sqrt{s} = 2.5$ TeV, we get from Fig.1a

$$0 \leq g_\pi \leq 1.4 \tag{46}$$

From Fig.1b we get at $\sqrt{s} = 3$ TeV a weaker limit

$$g_\pi \leq 1.8, \tag{47}$$

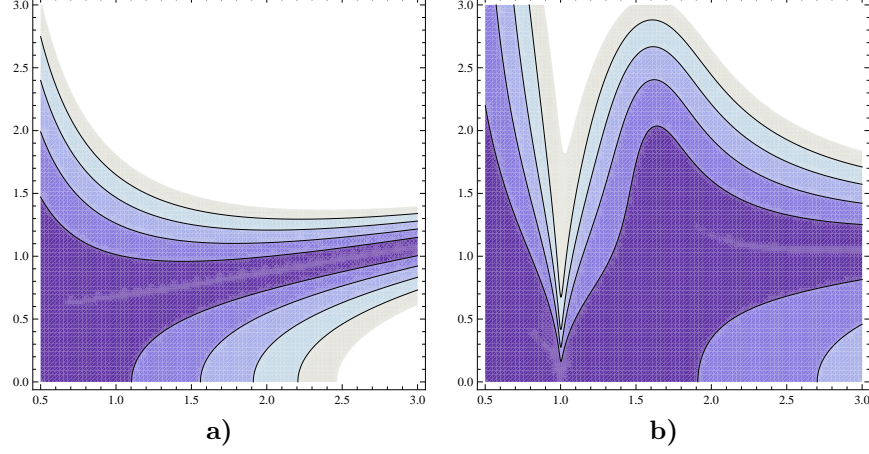


Figure 1: $\pi^+\pi^- \rightarrow \pi^+\pi^-$: Scenario 1. Contour plot of **a)** a_0 and **b)** a_1 partial wave as a function of \sqrt{s} (horizontal axis) and g_π (vertical axis). $g_V^t = g_A^t = 0.2, g_V^b = g_A^b = -0.2, M_{V^0} = 1$ TeV. Unitarity is violated in the 'white' area

the same as the limit from the resonance peak ($\sqrt{s} = 1$ TeV)

$$g_\pi \leq 1.8. \quad (48)$$

These limits depend on the quark couplings $g_V^t = g_A^t$ only indirectly, through the V^0 resonance width. As an illustration I show contour plots of a_0 and a_1 partial waves in Figs. 2a,b,c for $g_V^t = g_A^t = -g_V^b = -g_A^b = 0.02$ ($10\times$ smaller than in Fig.1). The a_0 partial wave (Fig.2a) has not changed (as compared with Fig.1a), demonstrating independence of the quark couplings. For a_1 partial wave (Fig.2b) things have not changed for $\sqrt{s} = 3$ TeV region (the limit of Eq. 47 still holds), however, the resonance peak limit at $\sqrt{s} = 1$ TeV (Fig.2b and Fig. 2c with a detailed view of the peak region) became much stronger than the limit of Eq.48:

$$g_\pi \leq 0.7, \quad (49)$$

indicating that for very small fermion couplings ($g_V^t = 0.02$ corresponds for the low energy limit $g'' = 10$ to $b_R \doteq -0.016$) the resonance peak unitarity limits can dominate over the $\sqrt{s} = 3$ TeV limits of Eqs. 45,46. For $g_V^t < 0.02$ it will become yet stronger.

Scenario 2 ($M_{V^0} = 1$ TeV). Only the resonance peak ($\sqrt{s} = 1$ TeV) limits change to ($g_V^t = 0.2, g_A^t = 0, g_V^b = -0.2, g_A^b = 0$)

$$g_\pi \leq 1.6 \quad (50)$$

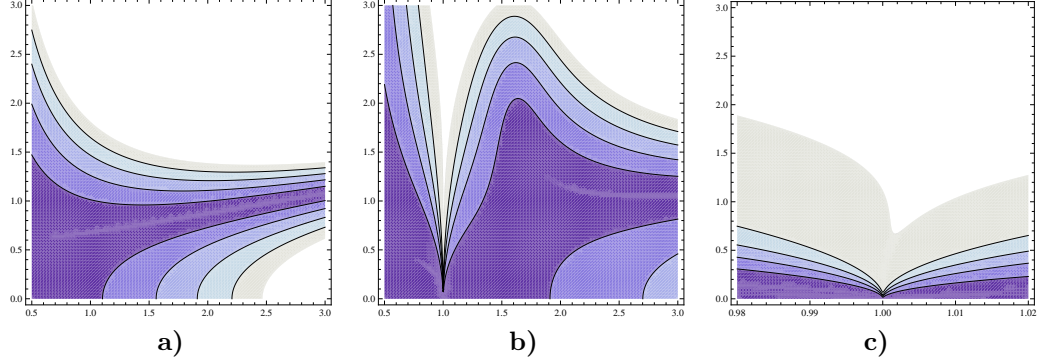


Figure 2: $\pi^+\pi^- \rightarrow \pi^+\pi^-$: Scenario 1. Contour plot of **a)** a_0 , **b)**, **c)** a_1 partial wave as a function of \sqrt{s} (horizontal axis) and g_π (vertical axis). $g_V^t = g_A^t = 0.02$, $g_V^b = g_A^b = -0.02$, $M_{V^0} = 1$ TeV. Unitarity is violated in the 'white' area. **c)** is a detailed view of the peak region from **b)**.

and to ($g_V^t = 0.02, g_A^t = 0, g_V^b = -0.02, g_A^b = 0$)

$$g_\pi \leq 0.5 \quad (51)$$

Scenario 3 ($M_{V^0} = 1$ TeV) yields the same results as scenario 2, *i.e.* compared to scenario 1 only the resonance peak ($\sqrt{s} = 1$ TeV) limits change to ($g_V^t = g_A^t = 0.2, g_V^b = g_A^b = 0$)

$$g_\pi \leq 1.6 \quad (52)$$

and to ($g_V^t = g_A^t = 0.02, g_V^b = g_A^b = 0$)

$$g_\pi \leq 0.5 \quad (53)$$

Summarizing all these limits, we conclude that the unitarity limit from $\pi^+\pi^- \rightarrow \pi^+\pi^-$ is

$$0 \leq g_\pi \leq 0.5 \quad (54)$$

valid for energies up to $\sqrt{s} = 2.5$ TeV and for quark couplings $g_V^t \geq 0.02$ (which corresponds for the low energy limit $g'' = 10$ to $b_R \leq -0.016$ in scenarios 1,3 and $b_R = b_L \leq -0.008$ in scenario 2).

In our model we get ($g'' = 10$)

$$g_\pi = \frac{M_{V^0}}{vg''} \doteq 0.41 \quad (M_{V^0} = 1 \text{ TeV}) \quad (55)$$

hence our choice of parameters (which respects low energy constraints) meets unitarity constraint.

3.2 $t\bar{t} \rightarrow t\bar{t}$

There are two Feynman diagrams, s-channel V^0 exchange and t-channel V^0 exchange, leading to 6 nonzero helicity amplitudes (found with */tt-tt.nb program which takes as input */dirac.m program developed by Miki; in $m_t/\sqrt{s} \rightarrow 0, p_3 \rightarrow E$ approximation) :

$$\begin{aligned}
\mathcal{M}^{+--+} &= -2(g_A^t + g_V^t)^2 \frac{s(\cos \theta/2)^2}{-M_{V^0}^2 + s + iM_{V^0}\Gamma_{V^0}} + 2(g_A^t + g_V^t)^2 \frac{s(\cos \theta/2)^2}{-M_{V^0}^2 - \frac{s(1-\cos \theta)}{2}} \\
\mathcal{M}^{-++-} &= -2(g_A^t - g_V^t)^2 \frac{s(\cos \theta/2)^2}{-M_{V^0}^2 + s + iM_{V^0}\Gamma_{V^0}} + 2(g_A^t - g_V^t)^2 \frac{s(\cos \theta/2)^2}{-M_{V^0}^2 - \frac{s(1-\cos \theta)}{2}} \\
\mathcal{M}^{+---} &= 2(-g_A^t{}^2 + g_V^t{}^2) \frac{s(\sin \theta/2)^2}{-M_{V^0}^2 + s + iM_{V^0}\Gamma_{V^0}} \\
\mathcal{M}^{-++-} &= \mathcal{M}^{+--+} \\
\mathcal{M}^{++++} &= 2(-g_A^t{}^2 + g_V^t{}^2) \frac{s}{-M_{V^0}^2 - \frac{s(1-\cos \theta)}{2}} \\
\mathcal{M}^{----} &= \mathcal{M}^{++++}
\end{aligned} \tag{56}$$

Partial waves and unitarity limits can be found in melo/SERVER/FYZIKA/MATHEMATICA/PARTIALWAVE/2010/tt-tt-gama1-2010-*.nb files. where * stands for a,a1 (scenario 1), b,b1 (scenario 2), c,c1 (scenario 3).

Scenario 1 ($M_{V^0} = 1$ TeV). For $g_V^t = g_A^t, g_V^b = g_A^b = -g_V^t, g_\pi = 0.2$ we get a contour plot of the only nonzero partial wave, a_1^{+--+} , in Fig.3.

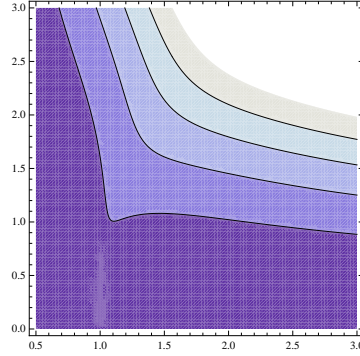


Figure 3: $t\bar{t} \rightarrow t\bar{t}$: Scenario 1. Contour plot of a_1^{+--+} partial wave as a function of \sqrt{s} (horizontal axis) and $g_V^t = g_A^t$ (vertical axis). $g_\pi = 0.2, M_{V^0} = 1$ TeV. Unitarity is violated in the 'white' area.

We conclude from Fig.3 that (constraint comes from $\sqrt{s} = 3$ TeV, *we do not*

have unitarity violation in the ρ resonance peak)

$$g_A^t = g_V^t \leq 2.0 \quad (M_\rho = 1 \text{ TeV}) \quad (57)$$

I have checked that this is valid also for $g_\pi = 0.02$ (Fig. 3 is independent of g_π).

Scenario 2 ($M_{V^0} = 1 \text{ TeV}$). For $g_A^t = g_A^b = 0, g_V^b = -g_V^t, g_\pi = 0.2$ we get 8 nonzero partial waves, see Fig.4. However, neither of them gives a limit for g_V^t

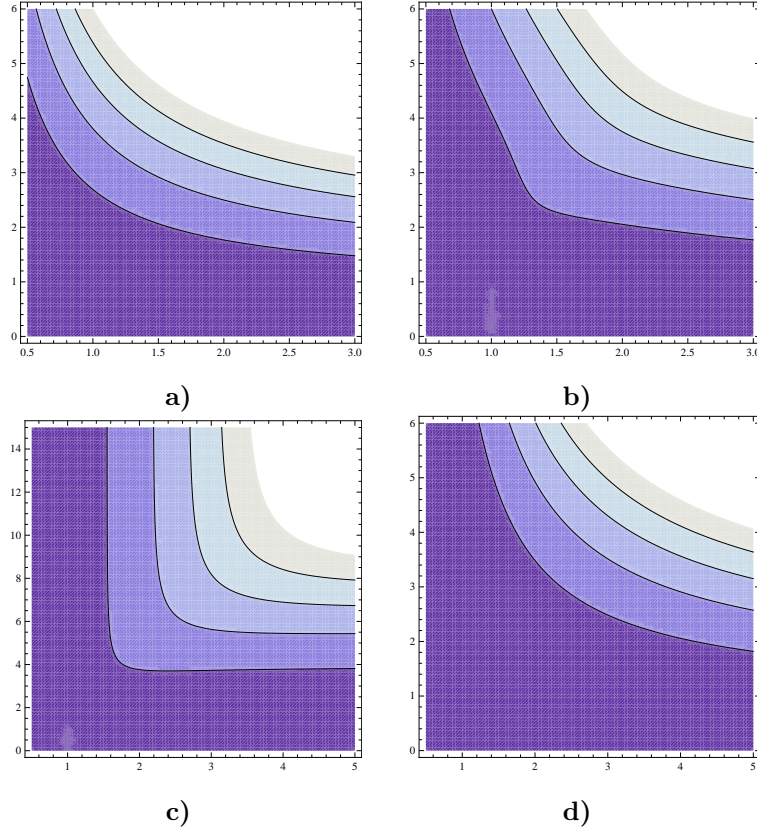


Figure 4: $t\bar{t} \rightarrow t\bar{t}$: Scenario 2. Contour plot of **a)** $a_0^{++++} = a_0^{----}$, **b)** $a_1^{+-+-} = a_1^{-+-+}$, **c)** $a_1^{+--+} = a_1^{-++-}$ and **d)** $a_1^{++++} = a_1^{----}$ partial waves as a function of \sqrt{s} (horizontal axis) and g_V^t (vertical axis). $g_\pi = 0.2, M_{V^0} = 1 \text{ TeV}$. Unitarity is violated in the 'white' area

better than Eq.57. I have checked that Fig.4 will not change for $g_\pi = 0.02$.

Scenario 3 ($M_{V^0} = 1 \text{ TeV}$). For $g_V^t = g_A^t, g_A^b = g_V^b = 0, g_\pi = 0.2$ we get again just one nonzero partial wave, a_1^{+-+-} , see Fig.5.

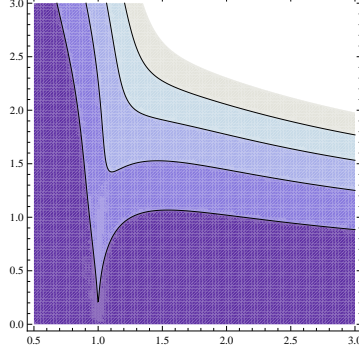


Figure 5: $t\bar{t} \rightarrow t\bar{t}$: Scenario 3. Contour plot of a_1^{+-+-} partial wave as a function of \sqrt{s} (horizontal axis) and $g_V^t = g_A^t$ (vertical axis). $g_\pi = 0.2$, $M_{V^0} = 1$ TeV. Unitarity is violated in the 'white' area.

The limit from here is the same as the one in Eq. 57. I have checked that Fig.5 will not change for $g_\pi = 0.02$.

In our model we get in scenarios 1 and 3 ($g_A^t = g_V^t, g'' = 10, b_L = 0, b_R = -0.1$)

$$g_V^t \doteq -\frac{g''}{8}b_R = 0.125 \leq 2.0 \quad (58)$$

To express unitarity limits directly in variables b_L, b_R , we show allowed regions in these parameters for $\sqrt{s} = 2.5$ TeV in Figs. 6a,b. We get from here

$$\begin{aligned} |b_L, b_R| &\leq 1.4 \\ |b_L, b_R| &\leq 0.15 \end{aligned} \quad (59)$$

for $g'' = 10$ and $g'' = 100$, respectively.

3.3 $\pi\pi \rightarrow t\bar{t}$

There are 4 nonzero helicity amplitudes (see my notes 8.3.04; in $m_t/\sqrt{s} \rightarrow 0, p_3 \rightarrow E$ approximation):

$$\begin{aligned} \mathcal{M}^{++} &= m_t \frac{\sqrt{s}}{v^2} + 2 \frac{m_t^3}{v^2 \sqrt{s}} + 2g_\pi g_V \frac{M_\rho}{v} m_t \frac{\sqrt{s}}{s - M_\rho^2 + iM_\rho \Gamma_\rho} \cos \theta \\ \mathcal{M}^{--} &= -\mathcal{M}^{++} \\ \mathcal{M}^{+-} &= g_\pi (g_V + g_A) \frac{M_\rho}{v} \frac{s}{s - M_\rho^2 + iM_\rho \Gamma_\rho} \sin \theta - 2 \frac{m_t^2}{v^2} \frac{(1 + \cos \theta)}{\sin \theta} \end{aligned}$$

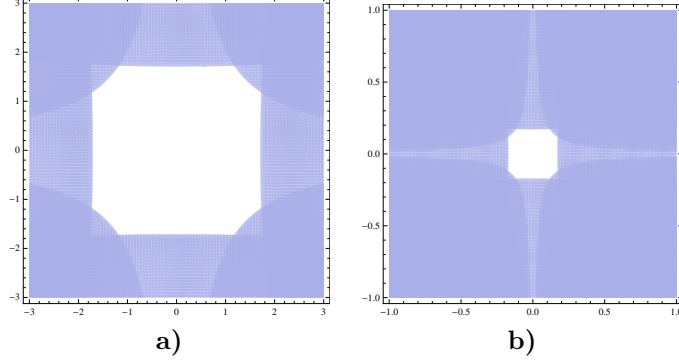


Figure 6: $t\bar{t} \rightarrow t\bar{t}$: Allowed regions (white) in the b_L (horizontal axis) vs b_R (vertical axis) parametric space for **a)** $g'' = 10$ and **b)** $g'' = 100$. All partial waves are included and superimposed. $M_{V^0} = 1$ TeV. Unitarity is violated in the 'blue' area.

$$\mathcal{M}^{-+} = g_\pi(g_A - g_V) \frac{M_\rho}{v} \frac{s}{s - M_\rho^2 + iM_\rho\Gamma_\rho} \sin\theta \quad (60)$$

Partial waves and unitarity limits can be found in melo/SERVER/FYZIKA/MATHEMATICA/PARTIALWAVE/2010/pipi-tt-gama1-2010-*.nb files. where * stands for a,a1,a2 (scenario 1), b,b1,b2 (scenario 2), c,c1,c2 (scenario 3).

Scenario 1 ($M_{V^0} = 1$ TeV). For $g_V^t = g_A^t, g_V^b = g_A^b = -g_V^t, g_\pi = 1.2$ we get contour (and LEGO) plots of $a_0^{++} = a_0^{--}, a_1^{++} = a_1^{--}$ and a_1^{+-} partial waves in Fig.7a,b,c.

The unitarity **is not violated** neither by a_0 nor a_1 for all 'reasonable' parameter space

$$\begin{aligned} g_\pi &\leq 1.2, \\ 0 &\leq g_V^t \leq 3, \\ 0.5 \text{ TeV} &\leq \sqrt{s} \leq 3 \text{ TeV} \end{aligned} \quad (61)$$

for $M_{V^0} = 1$ TeV. Scenarios 2 and 3 do not change these conclusions (the changes are minor and not significant - see the relevant *.nb files).

3.4 $t\bar{b} \rightarrow t\bar{b}$

There are two Feynman diagrams, s-channel V^+ exchange and t-channel V^0 exchange, leading to 6 nonzero helicity amplitudes (found with */tB-tB.nb program which takes as input */dirac.m program developed by Miki; in $m_t/\sqrt{s} \rightarrow$

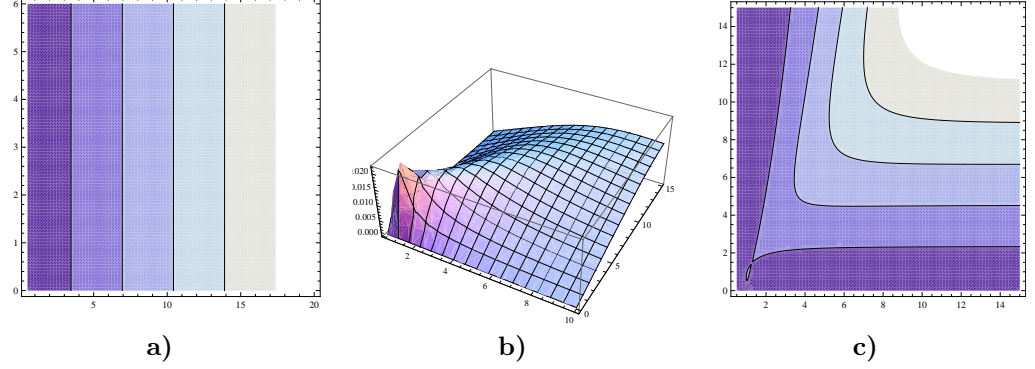


Figure 7: $\pi^+\pi^- \rightarrow t\bar{t}$: Scenario 1. Contour (and LEGO) plots of **a)** a_0^{++} , **b)** a_1^{+-} , **c)** a_1^{+-} partial wave as a function of \sqrt{s} (horizontal axis) and g_V^t (vertical axis). For LEGO plot **b)** the vertical axis shows the absolute value of the partial wave. $g_V^t = g_A^t$, $g_V^b = g_A^b$, $g_\pi = 1.2$, $M_{V^0} = 1$ TeV. Unitarity is violated in the 'white' area.

$0, p_3 \rightarrow E$ approximation) :

$$\begin{aligned}
\mathcal{M}^{++++} &= \frac{2s(g_A^{tb} + g_V^{tb})^2 \cos^2(\theta/2)}{-M_{V^+}^2 + s + i M_{V^+} \Gamma_{V^+}} + \frac{2s(g_A^b + g_V^b)(g_A^t + g_V^t) \cos^2(\theta/2)}{-M_{V^0}^2 - \frac{1}{2}s(1 - \cos \theta)} \\
\mathcal{M}^{-+++} &= \frac{2s(g_A^{tb} - g_V^{tb})^2 \cos^2(\theta/2)}{-M_{V^+}^2 + s + i M_{V^+} \Gamma_{V^+}} + \frac{2s(g_A^b - g_V^b)(g_A^t - g_V^t) \cos^2(\theta/2)}{-M_{V^0}^2 - \frac{1}{2}s(1 - \cos \theta)} \\
\mathcal{M}^{+---} &= \frac{2s(-g_A^{tb^2} + g_V^{tb^2}) \sin^2(\theta/2)}{-M_{V^+}^2 + s + i M_{V^+} \Gamma_{V^+}} \\
\mathcal{M}^{-++-} &= \frac{2s(-g_A^{tb^2} + g_V^{tb^2}) \sin^2(\theta/2)}{-M_{V^+}^2 + s + i M_{V^+} \Gamma_{V^+}} \\
\mathcal{M}^{++++} &= \frac{2s(g_A^b - g_V^b)(g_A^t + g_V^t)}{-M_{V^0}^2 - \frac{1}{2}s(1 - \cos \theta)} \\
\mathcal{M}^{----} &= \frac{2s(g_A^b + g_V^b)(g_A^t - g_V^t)}{-M_{V^0}^2 - \frac{1}{2}s(1 - \cos \theta)}
\end{aligned} \tag{62}$$

Partial waves and unitarity limits can be found in melo/SERVER/FYZIKA/MATHEMATICA/PARTIALWAVE/2010/tB-tB-gama1-2010-*.nb files. where * stands for a,a1 (scenario 1), b,b1 (scenario 2), c (scenario 3).

Scenario 1 ($M_{V^0} = 1$ TeV, $M_{V^+} = 1$ TeV). For $g_V^t = g_A^t$, $g_V^b = g_A^b = -g_V^t$, $g_A^{tb} = g_V^{tb}$, $g_V^{tb} = 2.g_V^t/\sqrt{2}$, $g_\pi = 0.2$, $g'_\pi = 0.2$ we get a contour plot of the only nonzero a_1^{+-} partial wave in Fig.8.

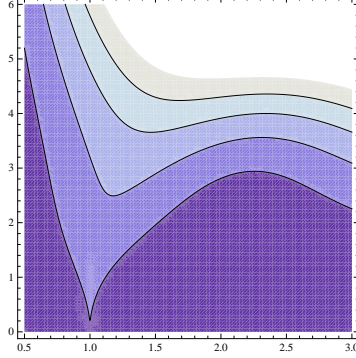


Figure 8: $t\bar{b} \rightarrow t\bar{b}$: Scenario 1. Contour plot of a_1^{+-+} partial wave as a function of \sqrt{s} (horizontal axis) and g_V^{tb} (vertical axis). $g_\pi = g'_\pi = 0.2$, $M_{V^0} = M_{V^+} = 1$ TeV. Unitarity is violated in the 'white' area.

We conclude from Fig. 8 that for energies $\sqrt{s} < 3$ TeV

$$g_V^{tb} \leq 4.4 \quad (63)$$

Fig. 8 will not change if we choose $g_\pi = g'_\pi = 0.02$.

Scenario 2 yields 8 nonzero partial waves, however, none of them gives a stricter limit than Eq. 59. Scenario 3 has all partial waves equal to zero.

To express unitarity limits directly in variables b_L, b_R , we show allowed regions in these parameters for $\sqrt{s} = 2.5$ TeV in Figs. 9a,b for $g'' = 10$ and $g'' = 100$, respectively. These limits are not stricter than the limits of Eq. 59.

References

- [1] L. Durand, J.L. Lopez: *Phys. Rev.* **D40** (1989), 207.
- [2] J. Horejsi: *Elektroslabe sjednoceni a stromova unitarita* (1993).

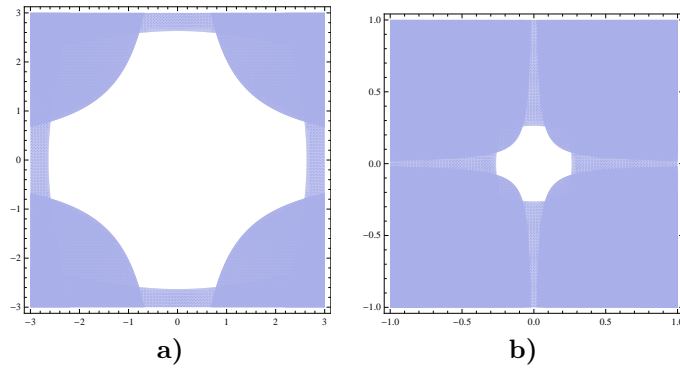


Figure 9: $\bar{t}\bar{b} \rightarrow t\bar{b}$: Allowed regions (white) in the b_L (horizontal axis) vs b_R (vertical axis) parametric space for **a)** $g'' = 10$ and **b)** $g'' = 100$. All partial waves are included and superimposed. $M_{V^0} = M_{V^+} = 1$ TeV. Unitarity is violated in the 'blue' area.